



# DIRECT NUMERICAL SIMULATION OF THE JET ATOMIZATION PROCESS OF SHEAR THINNING GEL FUEL

Kangbo Yang<sup>2</sup>, Yuqi Huang<sup>1</sup>, Weijuan Yang<sup>3</sup>, Shuai Wang<sup>4</sup>, Haiou Wang<sup>5</sup>, Jianren Fan<sup>6</sup>

<sup>1</sup> Corresponding Author. Department of Energy Engineering, Zhejiang University, Hangzhou, 310027, China. Tel.: +86 13867472242, E-mail: huangyuqi@zju.edu.cn

<sup>2</sup> Department of Energy Engineering, Zhejiang University, Hangzhou, E-mail: 12127067@zju.edu.cn

<sup>3</sup> Department of Energy Engineering, Zhejiang University, Hangzhou, E-mail: yangwj@zju.edu.cn

<sup>4</sup> Department of Energy Engineering, Zhejiang University, Hangzhou, E-mail: wshuai2014@zju.edu.cn

<sup>5</sup> Department of Energy Engineering, Zhejiang University, Hangzhou, E-mail: wanghaiou@zju.edu.cn

<sup>6</sup> Department of Energy Engineering, Zhejiang University, Hangzhou, E-mail: fanjr@zju.edu.cn

## ABSTRACT

Gel fuels have significant potential in aerospace applications. The shear-thinning behavior of gel fuel significantly impacts its atomization process. This study uses direct numerical simulation (DNS) with a coupled three-dimensional Volume-of-Fluid (VoF) and Lagrangian Particle Tracking (LPT) model to investigate the jet atomization of shear-thinning gel fuel (50 m/s, 0.6 mm injection diameter), comparing it with Newtonian fluid atomization. The gelatinized fuel is harder to atomize due to its higher viscosity. High-viscosity regions are concentrated in the jet core and shed in the jet direction, influenced by the velocity distribution within the liquid column. Shear-thinning fluids display unique dynamics: surface instability waves form earlier and primarily grow radially. In contrast, instability waves in Newtonian fluids grow radially while also developing in the direction opposite to the jet velocity. The high-viscosity core suppresses radial expansion, causing hole formation due to gas backflow and liquid film wrapping. A parabolic velocity inlet may optimize atomization by reducing the high-viscosity core. This study reveals how shear rate-viscosity coupling affects instability and fragmentation, providing insights for nozzle design and atomization efficiency.

**Keywords:** Direct numerical simulation; Instability waves; Shear thinning

## NOMENCLATURE

### Latin Capital Letters

$E$	[N]	force
$E_D$	[N]	drag force
$E_G$	[N]	gravity and buoyancy force
$E_{SRM}$	[N]	aerodynamic force

### Latin Lowercase Letters

$g$	[m/s <sup>2</sup> ]	gravitational acceleration
$k$	[Pa s <sup>n</sup> ]	consistency coefficient
$m$	[kg]	mass
$n$	[-]	power-law index
$p$	[Pa]	pressure
$t$	[s]	time
$u$	[m/s]	velocity
$x$	[m]	position

### Greek Symbols

$\alpha$	[-]	liquid volume fraction
$\dot{\gamma}$	[1/s]	shear rate
$\rho$	[kg/m <sup>3</sup> ]	density
$\mu$	[Pa s]	dynamic viscosity
$\eta_K$	[m]	Kolmogorov scale

### Other Symbols

$\underline{\sigma}$	[N]	surface tension force
$\phi_V$	[-]	Liquid Volume Retention Ratio
$\phi_S$	[-]	Interface Generation Rate
$Re$	[-]	Reynolds number
$We$	[-]	Weber number
$Oh$	[-]	Ohnesorge number
$V_{sim}$	[m <sup>3</sup> ]	simulated liquid volume
$V_{theory}$	[m <sup>3</sup> ]	theoretical volume of the unatomized cylindrical liquid jet
$S_{sim}$	[m <sup>2</sup> ]	simulated surface area of the liquid jet
$S_{theory}$	[m <sup>2</sup> ]	surface area of the unbroken liquid jet

### Subscripts

$g$	gas phase
$l$	liquid phase
$p$	parcel
$max$	maximum
$min$	minimum

## 1. INTRODUCTION

Gel fuels, characterized by their unique shear-thinning behavior, have emerged as a promising candidate for aerospace propulsion systems due to their dual advantages of liquid-like flowability and solid-like storability. The atomization process of gel fuels directly affects combustion efficiency and thrust performance. Unlike Newtonian fluids, the viscosity of shear-thinning gels decreases significantly under high shear rates (e.g., during injection through narrow nozzles), complicating the atomization dynamics. However, the interplay between shear-thinning rheology, jet instability, and atomization patterns remains poorly understood. Traditional experimental methods struggle to resolve transient interfacial dynamics and localized viscosity variations, while conventional numerical approaches (e.g., RANS or LES [1]) often fail to capture the multiscale interactions between turbulent vortices and non-Newtonian fluid interfaces. Direct Numerical Simulation (DNS), capable of resolving all turbulent scales without modeling assumptions, offers a powerful tool to unravel the intrinsic mechanisms governing shear-thinning jet atomization.

Current research on jet atomization primarily focuses on Newtonian fluids. Menard et al. [2] combined the VOF, Level Set method, and GFM method to resolve the droplet formation and interface fragmentation in the primary breakup of high-speed liquid jets via DNS. The data obtained from DNS further validated and advanced the ELSA model [3]. Shinjo et al. [4] employed DNS with the combination of Level Set and VOF methods to study primary atomization phenomena of high-speed liquid jets under high-pressure conditions, revealing that the main droplet formation mode is driven by capillary waves. The Weber number significantly influences the size of ligaments and droplets in atomization. Further studies, conducted at high grid resolution, explored the formation of a conical structure at the tip of the jet and its subsequent atomization process. They also highlighted that droplet formation could transition from a short-wave mode to a long-wave mode under the stretching effect of the gas [5]. Research on intermittent diesel injection atomization processes also revealed that the surface instability of the liquid core is primarily induced by the gas-phase TS instability mode, with initial instability being two-dimensional, which evolves into three-dimensional instability over time. Most of these studies, however, did not consider the impact of nozzle perturbations on jet atomization. Jiao et al. [6] used DNS to study the effects of different liquid-gas density ratios and nozzle sizes on the turbulent fluctuation effects in diesel jets. Their findings showed that turbulent fluctuations promoted the evolution from a columnar liquid flow to an irregular droplet cluster, with higher gas density and smaller nozzle diameter accelerating this process. Salvador

et al. [7] used DNS to investigate the effects of turbulent inflow conditions on the primary atomization process at low Reynolds numbers. They found that turbulence length scales significantly affected droplet fragmentation patterns, with higher turbulence intensity promoting earlier atomization and shorter core lengths. Additionally, Cialesi-Esposito et al. [8] compared the effects of isotropic (SBC) and anisotropic (MBC) turbulent conditions on spray breakup using DNS. Their results indicated that while the total number of droplets generated differed under different turbulence conditions, the overall atomization dynamics remained consistent, and larger turbulent structures more readily promoted atomization and the formation of smaller droplets. Srinivasan et al. [9] studied the influence of different jet velocity profiles on primary breakup using DNS, revealing that parabolic velocity profiles had deeper penetration and more pronounced surface wave changes, leading to more fragmentation features.

While DNS provides unparalleled resolution of interfacial dynamics and turbulent interactions, its computational cost remains prohibitive for industrial-scale applications. To reduce computational costs, some researchers have adopted Eulerian-Lagrangian coupled methods to simulate atomization processes, significantly reducing computational time while maintaining accuracy [10, 11].

In the study of shear-thinning fluid jet atomization, Ertl et al. [12] used DNS to investigate the primary breakup of shear-thinning fluid jets with different velocity profiles, emphasizing that the choice of velocity profile had a more significant impact on breakup than the shear-thinning properties themselves. Zhao et al. [13] employed a VOF-DNS coupled method to study the spray characteristics of power-law biodiesel, finding that shear-thinning fluids exhibited jet breakup patterns similar to Newtonian fluids, with higher Reynolds numbers and gas densities accelerating the breakup process. Abdelsayed et al. [14] conducted DNS to study the primary atomization process of Newtonian and shear-thinning fluids, finding that droplets generated by shear-thinning fluids were more fibrous and exhibited higher surface irregularities. However, numerical simulations of shear-thinning fluid jet atomization are still limited, with few studies comparing simulation results with experimental data and insufficient understanding of the unique atomization morphology of shear-thinning fluids.

This study adopts a three-dimensional coupled Volume-of-Fluid and Lagrangian Particle Tracking (VOF-LPT) model [10], combined with Direct Numerical Simulation (DNS), to analyze the jet atomization process of shear-thinning fluids. Through a quantitative comparison of atomization morphology and experimental observations [15], the numerical model's ability to capture interfacial

evolution is validated. A comparison between shear-thinning and Newtonian fluid jet atomization highlights the more frequent wave structures and internal hole formation observed in shear-thinning fluid atomization, providing valuable insights for enhancing shear-thinning fluid jet atomization.

## 2. NUMERICAL SIMULATION METHODOLOGY

### 2.1. Governing equation

The simulations in this study were performed using a two-phase flow solver in OpenFOAM, based on the Volume-of-Fluid (VOF) and Lagrangian Particle Tracking (LPT) coupling method. The governing equations for the two-phase flow consist of mass and momentum conservation laws:

$$\nabla \cdot \underline{u} = 0 \quad (1)$$

$$\frac{\partial \rho \underline{u}}{\partial t} + \nabla \cdot (\rho \underline{u} \underline{u}) = -\nabla p + \nabla \cdot [\mu (\nabla \underline{u} + \nabla \underline{u}^T)] + \underline{f}_\sigma \quad (2)$$

where the  $\rho$  and  $\mu$  are given by the following relations:

$$\rho = \alpha \rho_l + (1 - \alpha) \rho_g \quad (3)$$

$$\mu = \alpha \mu_l + (1 - \alpha) \mu_g \quad (4)$$

and  $\underline{f}_\sigma$  is modeled via the CSF approach .

Interface dynamics during the primary breakup are resolved using a Volume-of-Fluid (VOF) method with geometric interface reconstruction via the isoAdvector method. The phase fraction transport equation is given by:

$$\frac{\partial \alpha}{\partial t} + \nabla \cdot (\alpha \underline{u}) = 0 \quad (5)$$

The Lagrangian Particle Tracking (LPT) method is used to track the movement of Lagrangian particles within the computational domain:

$$\frac{d \underline{x}_p}{dt} = \underline{u}_p \quad (6)$$

$$m_p \frac{d \underline{u}_p}{dt} = \underline{F}_D + \underline{F}_G + \underline{F}_{SRM} \quad (7)$$

$$\underline{F}_G = m_p \left( 1 - \frac{\rho_g}{\rho_l} \right) \underline{g} \quad (8)$$

where  $\underline{F}_D$  follows Schiller-Naumann correlation, and  $\underline{F}_{SRM}$  accounts for secondary breakup via the Reitz-Diwakar model. The coupling between VOF and

LPT is detailed in the reference [10], and will not be repeated here.

For the viscosity of shear-thinning fluids, this study uses a modified power-law model:

$$\mu_l = \min(\mu_{l,max}, \max(\mu_{l,min}, k \cdot \dot{\gamma}^{n-1})) \quad (9)$$

### 2.2. Boundary Conditions

In this study, numerical simulations are conducted for the jet atomization process of JP-10 solution (Newtonian fluid) and its shear-thinning modified solution [16]. Both solutions have a density of  $970 \text{ kg/m}^3$ , surface tension coefficient of  $0.032 \text{ N/m}$ , and Newtonian fluid has a constant kinematic viscosity of  $1.2 \times 10^{-6} \text{ m}^2/\text{s}$ . For the shear-thinning solution, the parameters are  $\mu_{l,max} = 1.2 \times 10^{-2} \text{ m}^2/\text{s}$ ,  $\mu_{l,min} = 1.2 \times 10^{-6} \text{ m}^2/\text{s}$ ,  $k = 0.012 \text{ Pa s}^n$ ,  $n = -0.132$ . The power-law index  $n$  of the shear-thinning solution is less than 0, indicating that this gel solution has a stronger thinning ability than typical shear-thinning fluids ( $0 < n < 1$ ) [16]. The jet breakup process can be divided into four regions based on different Reynolds and Ohnesorge numbers [17]. In this study, the viscosity of shear-thinning fluids is not constant, making it impossible to directly calculate the Reynolds number. Previous studies have used a modified Reynolds number for power-law fluids [18], but this method is not applicable in this study due to the  $n < 0$  for the shear-thinning fluid. In this study, the dimensionless parameters are calculated using the average  $\mu_l$  at the nozzle cross-section, yielding  $Re = 22058$ , with  $We = 45469$  and  $Oh = 0.0097$  calculated subsequently. Based on the reference [17], the jet flow in this study falls into the atomization region. The computational domain is set as a rectangular region of  $6D \times 6D \times 25D$ , the nozzle length is  $1 \text{ mm}$ , and the initial jet velocity is  $50 \text{ m/s}$ . The boundary conditions include a velocity inlet, pressure outlet (at atmospheric pressure), and no-slip wall conditions. During the calculation, the maximum Courant number is kept below 0.3 to ensure numerical stability.

## 3. NUMERICAL SIMULATION VALIDATION AND GRID INDEPENDENCE ANALYSIS

This study employs dynamic adaptive mesh refinement (AMR) techniques to simulate the jet atomization process. Four different grid resolutions were tested, with minimum grid sizes of  $20 \text{ }\mu\text{m}$ ,  $15 \text{ }\mu\text{m}$ ,  $10 \text{ }\mu\text{m}$ , and  $7.5 \text{ }\mu\text{m}$ . To evaluate the results, the following metrics were defined based on the liquid phase volume fraction and interface surface area:

$$\varphi_v = \frac{V_{sim}}{V_{theory}} \times 100\% \quad (10)$$

$$\varphi_S = \frac{S_{sim}}{S_{theory}} \times 100\% \quad (11)$$

Figures 1 and 2 show the variation of  $\varphi_V$  and  $\varphi_S$  with the number of grids. It can be seen that as the grid size is refined from  $20 \mu m$  to  $7.5 \mu m$ : The liquid volume retention ratio increases from 98.35% to 99.65%, indicating that the finer grid significantly reduces numerical diffusion at the interface. The interface generation rate shows a growth trend consistent with the physical mechanism of surface area increase due to droplet breakup during atomization. Moreover, the fluctuation amplitude for the  $7.5 \mu m$  grid is similar to that for the  $10 \mu m$  grid, suggesting that the grid resolution is sufficient to capture the interface instability.

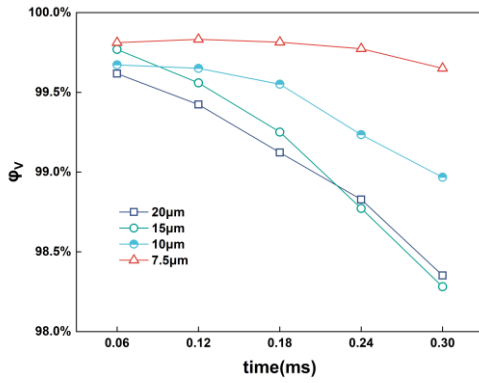


**Figure 1. Time-dependent variation of  $\varphi_V$  under different grid sizes**

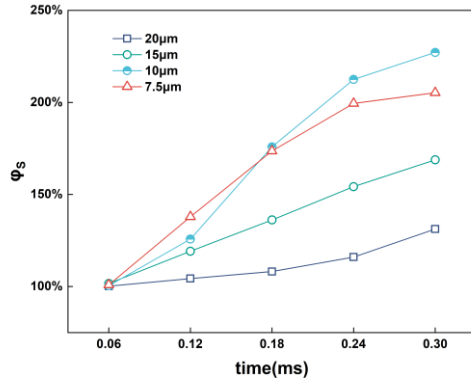
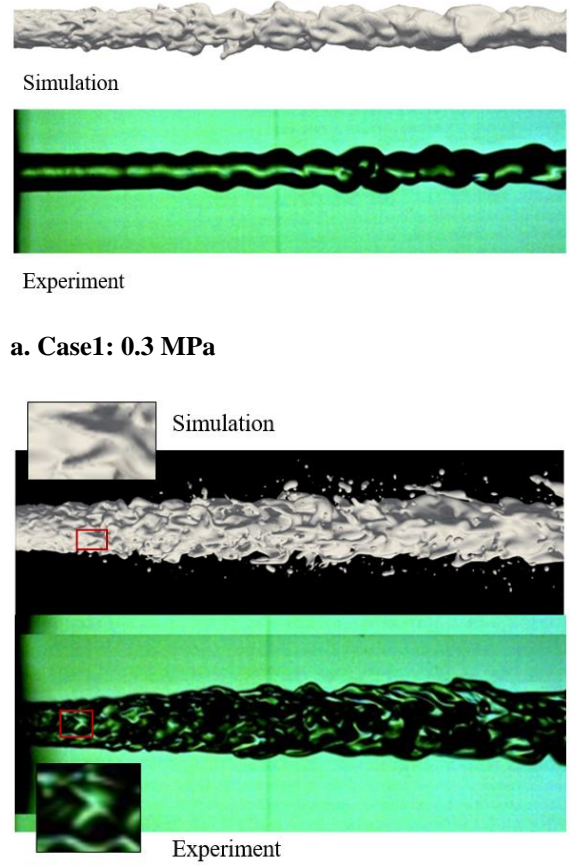


**Figure 2. Time-dependent variation of  $\varphi_S$  under different grid sizes**

Based on these analyses, a grid size of  $7.5 \mu m$  was selected as the final grid resolution. This size is of the same order of magnitude as the theoretical Kolmogorov scale ( $\eta_K=1.2\mu m$ ) and satisfies the sensitivity requirements for resolution in interface-dominated atomization processes. Additionally, the simulation results were validated by comparing the jet morphology with experimental results from the reference [15], as shown in Figure 3. The simulation conditions for the verification case are as follows:

Case 1.  $0.3 \text{ MPa}$ , velocity  $22.32 \text{ m/s}$ ; Case 2:  $0.6 \text{ MPa}$ , velocity  $31.22 \text{ m/s}$ .



**b. Case2: 0.6 MPa**

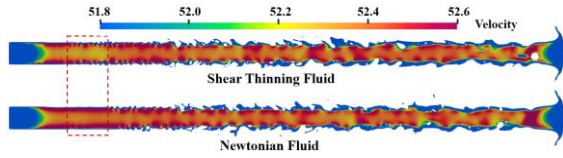
**Figure 3. Comparison of experimental and simulation results**

Under the  $0.3 \text{ MPa}$  condition, the simulated results successfully capture the jet column structure, resembling a helical distortion, which aligns with experimental observations. For the  $0.6 \text{ MPa}$  condition, the jet surface shape is more complex, and the jet is no longer a simple cylindrical form. The simulated results capture the expansion of the liquid column under these conditions, and the typical V-shaped wave structure observed in experiments is also reproduced. Therefore, it can be concluded that the simulation method used in this study is capable of accurately capturing the atomization structure in shear-thinning fluid jet atomization processes.

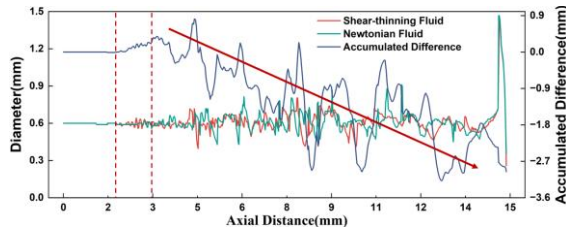
#### 4. RESULTS AND ANALYSIS

Figure 4 presents the liquid column cross-sections of Newtonian fluid and its shear-thinning solution at  $3 \times 10^{-4} \text{ s}$ . It is evident that the surface instability waves of the non-Newtonian fluid appear closer to the nozzle, and large voids are more likely to form inside the liquid column. To further explore the differences between the shear-thinning fluid and

Newtonian fluid jets, the variations in liquid column diameter with axial distance, as well as the cumulative differences between the two fluids, were statistically analyzed, as shown in Figure 5. It can be observed that the cumulative difference is initially greater than 0, further indicating that surface instability waves appear earlier in the non-Newtonian fluid. As the axial distance increases, the cumulative difference shows a gradual decline, suggesting that Newtonian fluids expand more easily in the radial direction. This may be because the high-viscosity region in the center of the non-Newtonian liquid column inhibits this process.



**Figure 4. Liquid column cross-sections of Newtonian fluid and shear-thinning fluid at  $3 \times 10^{-4}$  s.**



**Figure 5. Variations in liquid column diameter with axial distance and cumulative differences between shear-thinning fluid and Newtonian fluid jets**

As shown in Figure 6, the high-viscosity region of the shear-thinning fluid (indicated by the yellow area, where viscosity  $> 2.4 \times 10^{-6} \text{ m}^2/\text{s}$ ) is concentrated in the core of the liquid column and is primarily influenced by the velocity distribution within the liquid column. Near the nozzle, the distribution of surface instability waves causes the formation of intermittently distributed high-speed zones within the liquid column. The presence of these high-speed zones leads to corresponding arc-shaped depressions in the high-viscosity region, which is the main factor influencing the shape of the high-viscosity region in the radial direction. The shedding and separation of the high-viscosity region in the axial direction of the jet are mainly influenced by the axial velocity gradient. Despite the relatively small velocity difference within the liquid column (compared to the jet velocity), it still results in the continuous shedding of the high-viscosity region along the jet direction.

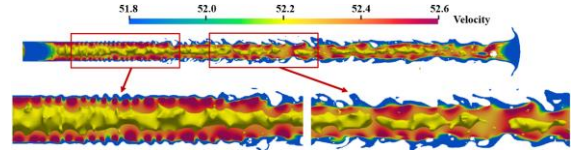


**Figure 6. Distribution of high-viscosity regions in the shear-thinning fluid jet and their correlation with velocity distribution and surface instability waves**

In the study by Balaji et al. [9], it was found that for Newtonian fluids, a flat velocity distribution at the nozzle produces the highest degree of atomization, while a parabolic velocity distribution exhibits the best penetration performance and results in the fastest reduction of liquid column diameter. Thus, it can be inferred that for shear-thinning fluids, using a parabolic velocity inlet could reduce the high-viscosity region in the liquid core, potentially enhancing the atomization process.

To further compare the different behaviors of shear-thinning and Newtonian fluids in jet atomization, Figure 7 shows the jet structures of both fluids at  $t = 3 \times 10^{-4}$  s. It can be observed that, compared to the Newtonian fluid, the surface of the shear-thinning fluid jet is more prone to generating instability wave structures perpendicular to the axial direction of the liquid column. Such phenomena are observed at both the neck and middle regions of the jet liquid column.

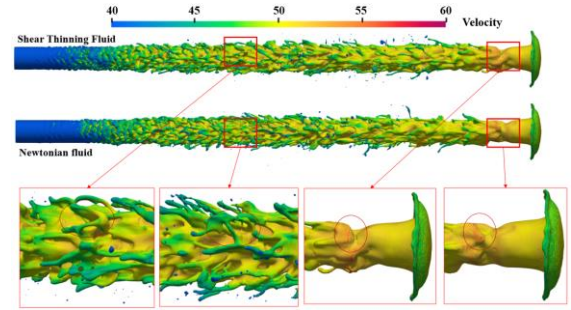


**Figure 7. Jet structures of shear-thinning and Newtonian fluids at  $3 \times 10^{-4}$  s**

To explore the reasons behind this phenomenon, the development of surface instability wave structures for both fluids was tracked, as shown in Figure 8. For the shear-thinning fluid, the instability waves on the liquid column surface initially appear as large V-shaped structures. Over time, these large V-shaped structures transition into smaller continuous V-shaped waves, which then grow radially along the liquid column. As time progresses further, the connections between the continuous V-shaped structures break, and the V-shaped structures continue to develop radially, while the ends of the instability waves stretch along the axial direction of the liquid column, reaching their final form.



In contrast, for the Newtonian fluid, the instability waves initially also take the form of large V-shaped structures, which gradually transform into smaller V-shaped waves. However, unlike the shear-thinning fluid, the instability waves on the surface of the Newtonian fluid grow radially while simultaneously tilting in the direction opposite to the jet flow. This results in the small V-shaped structures eventually evolving into liquid filaments.

The primary cause of this difference is the distribution of high-viscosity regions in the core of the shear-thinning fluid. Higher viscosity suppresses the growth of instability waves in the opposite direction of the jet. Additionally, previous studies have shown that the viscosity gradient within the fluid promotes instability propagation along the gradient [19]. In this study, the viscosity gradient in the shear-thinning fluid jet promotes the radial propagation of instability waves.

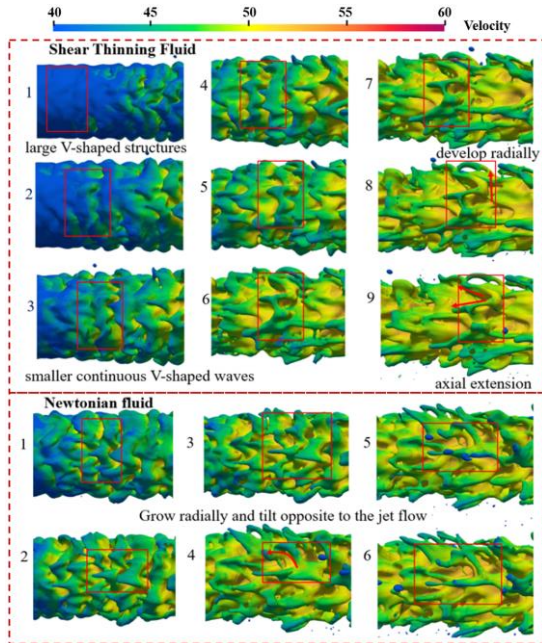


**Figure 8. Development of surface instability waves in shear-thinning and Newtonian fluids**

The unique wave structure exhibited by shear-thinning fluids during jet atomization is likely the main reason for the frequent formation of voids inside the liquid core. Figure 9 illustrates the formation process of a void structure in the shear-thinning fluid jet atomization. Initially, the void structure appears as a continuous V-shaped instability wave. As time progresses, the V-shaped instability wave grows radially along the liquid column. The incoming air flows past the continuous V-shaped structure and recirculates, generating a void on the liquid column surface. As time goes on, the gas recirculated through the continuous V-shaped structure enters the void, which causes the void to expand, penetrating deeper into the liquid core.

Simultaneously, the liquid film on the upper surface of the void moves in the opposite direction to the jet flow, ultimately encapsulating the void and forming an internal hole.

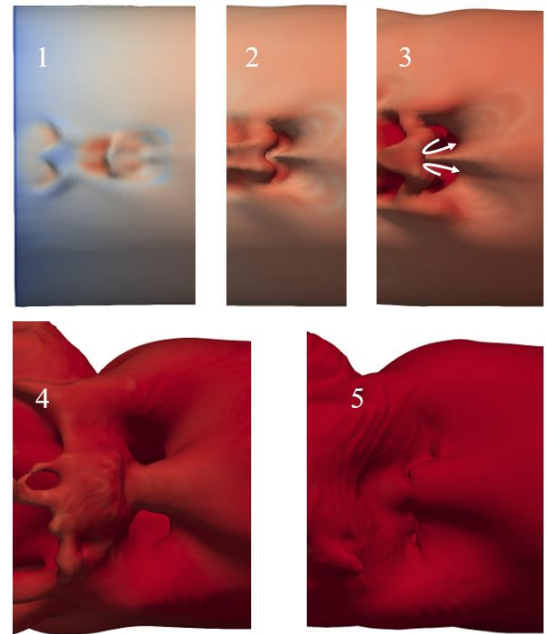


**Figure 9. Formation process of a void structure in shear-thinning fluid jet atomization, showing the growth and expansion of the void within the liquid core**

## 5. SUMMARY

This study investigates the jet atomization of shear-thinning gel fuels using direct numerical simulation (DNS) with a coupled three-dimensional Volume-of-Fluid (VOF) and Lagrangian Particle Tracking (LPT) model. The simulation results were validated through comparison with experimental observations, and key differences between shear-thinning and Newtonian fluids in atomization were highlighted.

**Effect of Velocity Distribution on Viscosity:** In shear-thinning fluids, high-viscosity regions are concentrated in the liquid core. The viscosity distribution is influenced by both the surface instability waves and the velocity distribution within the liquid column, which significantly affects the atomization behavior.

**Unique Structure Due to Viscosity Distribution:** The high viscosity in the core of the shear-thinning fluid leads to the development of surface instability waves that form earlier and grow radially. In contrast, Newtonian fluids exhibit instability waves that grow radially and also tilt in the opposite direction of the jet flow.

**Formation of Voids:** The instability waves in shear-thinning fluids contribute to the formation of internal voids within the liquid core. The voids are

primarily driven by air backflow, which deepens and expands the holes within the liquid column.

In conclusion, this study provides insights into the atomization mechanisms of shear-thinning fluids, highlighting the influence of viscosity distribution and the resulting unique structural formations. These findings, along with comparisons between shear-thinning and Newtonian fluids, offer valuable implications for improving atomization processes in gel fuel applications.

## ACKNOWLEDGEMENTS

This work is supported by the National Natural Science Foundation of China (Grant No: U2341283). We are grateful for this.

## APPENDICES

## REFERENCES

- [1] Abdelsayed M, Hasslberger J, Ertl M, Weigand B, Klein M. Toward large eddy simulation of shear-thinning liquid jets: A priori analysis of subgrid scale closures for multiphase flows. *Physics of Fluids* (1994). 2024;36(8).
- [2] Ménard T, Tanguy S, Berlemont A. Coupling level set/VOF/ghost fluid methods: Validation and application to 3D simulation of the primary break-up of a liquid jet. *International Journal of Multiphase Flow*. 2007;33(5):510-24.
- [3] Lebas R, Menard T, Beau PA, Berlemont A, Demoulin FX. Numerical simulation of primary break-up and atomization: DNS and modelling study. *International Journal of Multiphase Flow*. 2009;35(3):247-60.
- [4] Shinjo J, Umemura A. Simulation of liquid jet primary breakup: Dynamics of ligament and droplet formation. *International Journal of Multiphase Flow*. 2010;36(7):513-32.
- [5] Shinjo J, Umemura A. Detailed simulation of primary atomization mechanisms in Diesel jet sprays (isolated identification of liquid jet tip effects). *Proceedings of the Combustion Institute*. 2011;33(2):2089-97.
- [6] Jiao D, Zhang F, Du Q, Niu Z, Jiao K. Direct numerical simulation of near nozzle diesel jet evolution with full temporal-spatial turbulence inlet profile. *Fuel* (Guildford). 2017;207:22-32.
- [7] Salvador FJ, S. R, Crialesi-Esposito M, Blanquer I. Analysis on the effects of turbulent inflow conditions on spray primary atomization in the near-field by direct numerical simulation. *International Journal of Multiphase Flow*. 2018;102:49-63.
- [8] Crialesi-Esposito M, Gonzalez-Montero LA, Salvador FJ. Effects of isotropic and anisotropic turbulent structures over spray atomization in the near field. *International Journal of Multiphase Flow*. 2022;150:103891.
- [9] Srinivasan B, Sinha A. Primary breakup of liquid jet—Effect of jet velocity profile. *Physics of Fluids* (1994). 2024;36(3).
- [10] M. Heinrich, R. Schwarze. 3D-coupling of volume-of-fluid and Lagrangian particle tracking for spray atomization simulation in OpenFOAM. *SoftwareX*, 11 (2020), Article 100483
- [11] Chéron V, Brändle de Motta, Jorge César, Ménard T, Poux A, Berlemont A. A coupled Eulerian interface capturing and Lagrangian particle method for multiscale simulation. *Computers & Fluids*. 2023;256:105843.
- [12] Ertl M, Weigand B. Analysis methods for direct numerical simulations of primary breakup of shear-thinning liquid jets. *Atomization and Sprays*. 2017;27(4):303-17.
- [13] Zhao L, Jiao D, Xie X, Jiao K, Peng Z, Du Q. Direct numerical simulation of primary breakup for power-law biodiesel sprays. *Energy Procedia*. 2019;158:612-8.
- [14] Abdelsayed M, Trautner E, Berchtenbreiter J, Klein M. Primary atomization of shear-thinning liquid jets: a direct numerical simulation study. *Scientific Reports*. 2024;14(1):23896-15.
- [15] Guo JP, Bai FQ, Chang Q, Du Q. Investigation on asymmetric instability of cylindrical power-law liquid jets. *Energies* (Basel). 2019;12(14):2785.
- [16] Cao J, Pan L, Zhang X, Zou J. Physicochemical and Rheological Properties of Al/JP-10 Gelled Fuel. *Hanneng Cailiao = Chinese Journal of Energetic Materials*. 2020(5):382.
- [17] Csizmadia P, Till S, Hős C. An experimental study on the jet breakup of Bingham plastic slurries in air. *Experimental Thermal and Fluid Science*. 2019;102:271-8.
- [18] Csizmadia P, Hős C. CFD-based estimation and experiments on the loss coefficient for Bingham and power-law fluids through diffusers and elbows. *Computers & Fluids*. 2014;99:116-23.
- [19] Burghilea T, Wielage-Burchard K, Frigaard I, Martinez DM, Feng JJ. A novel low inertia shear flow instability triggered by a chemical reaction. *Physics of Fluids* (1994). 2007;19(8):083102,083102-13.